PCCP

Physical Chemistry Chemical Physics

Accepted Manuscript

This article can be cited before page numbers have been issued, to do this please use: A. G. Ichert and W. Barford, *Phys. Chem. Chem. Phys.*, 2026, DOI: 10.1039/D6CP01090C.

ROYAL SOCIETY OF CHEMISTRY

rsc.li/pccp

View Article Online
DOI: 10.1039/D6CP01090C

Triplet-Pair Character of the 2^1A_g Dark State of Polyenes

Alexandru G. Ichert
Department of Chemistry, Physical and Theoretical Chemistry Laboratory,
University of Oxford, Oxford, OX1 3QZ, UK and
Linacre College, University of Oxford, Oxford, OX1 3JA, UK[*]

William Barford
Department of Chemistry, Physical and Theoretical Chemistry Laboratory,
University of Oxford, Oxford, OX1 3QZ, UK and
Balliol College, University of Oxford, Oxford, OX1 3BJ, UK[†]

(Dated: June 11, 2026)

View Article Online
DOI: 10.1039/D6CP01090C

Abstract

We define and calculate the triplet-pair population of the 2^1A_g dark state in polyenes, as predicted by the π-electron Pariser-Parr-Pople (PPP) model, for chains of 8 to 14 C-atoms and Coulomb interaction parameter between 4-14 eV. Our definition of the triplet-pair population is motivated by a two-particle model of the 2^1A_g state. We use DMRG to solve the PPP model and we exploit the MPS representation of the DMRG wavefunction to compute the triplet-pair population. Using our results for short chain sizes, we predict a finite-size scaling value of the triplet-pair population of ca. 75% for realistic Coulomb interactions for polyene chains. Our results agree with other theoretical work on the doubly-excited character of polyenes, and represents further evidence that the 2^1A_g state is predominantly triplet-pair in character - with implications for singlet fission mechanisms in polyenes.

I. INTRODUCTION

The 2^1A_g dark state in polyenes has been of interest to researchers for over 50 years [1, 2]. There is general agreement to its mixed triplet-pair and charge-transfer exciton character in linear π-conjugated systems [1, 3–6], although limited effort has been directed towards quantifying the doubly-excited character [5, 7–10].

In 1972, Schulten and Karplus were the first to predict the triplet-pair (or bimagnon) character of the 2^1A_g state [1]; they showed that inclusion of doubly-excited determinants reproduced the relative energy ordering of the dark and bright states observed experimentally [2]. In 1976, Schulten et al. [11] further investigated the nature of the dark state and identified that double excitations make the dominant contribution to this wavefunction. Ten years later, Hayden and Mele compared the relaxed lattice configurations for the 2^1A_g state with that of two 1^3B_u states and noted a striking resemblance between the two for a chain of 16 C-atoms [12]. Further significant theoretical contributions were made in 1987 by Tavan and Schulten [13], who showed that covalent excitations are combinations of triplet excitations in long polyenes. Importantly, the lowest covalent state, namely the 2^1A_g state, has a bond structure described by a pair of neutral soliton-antisoliton pairs, or equivalently

---

* alexandru.ichert@chem.ox.ac.uk
† william.barford@chem.ox.ac.uk

View Article Online
DOI: 10.1039/D6CP01090C

a triplet-pair (where each triplet has a neutral soliton-antisoliton structure). Additional evidence for the four-soliton structure of the dark state in long polyenes was provided by Barford et al. [14, 15] for chains of up to 50 ethylene dimers.

Chandross et al. [3] used a diagrammatic exciton-basis valence bond description of polyenes to investigate the low-lying eigenstates of short chains. Their work showed that the 2^1A_g state is best referred to as a mixture of triplet-pair and charge-transfer exciton components. Likewise, Valentine et al. [6] calculated the exciton wavefunction of the 2^1A_g state and showed that it corresponds to the lowest member of a family of electron-hole excitations, which they named the "$2A_g$-family" of states. They concluded that the dark state is a linear combination of odd-parity charge-transfer excitons and $T_1 \otimes T_1$ (i.e., $1^3B_u \otimes 1^3B_u$) triplet-pairs. The hybridization between the exciton and triplet-pair components was investigated in more detail by Barford [5], who showed that the coupling between the two subspaces, mediated by a one-electron transfer between neighbouring triplets, was responsible for the strong binding of the triplet-pair.

More recently, do Casal et al. [7] used a definition of excited state character based on the one-electron transition density matrices to show that the optically allowed 1^1B_u state is almost exclusively singly-excited in character, whereas the 2^1A_g state exhibits large multiply-excited contributions with respect to the ground state. Chagas et al. [8] performed a similar calculation on polyenes of 6, 8, 10 and 12 C-atoms and observed that the doubly-excited character of the 2^1A_g state was above 50% in all cases, which increases with increasing chain size. This result complements the previous findings of Starcke et al. [9], who calculated the population of doubly-excited configurations in the 2^1A_g state of chains of two to six ethylene dimers to be ca. 80%. Furthermore, similar results were obtained by Boguslawski [10] who used a pair coupled-cluster double (pCCD) method to calculate the double excitation contribution to the 2^1A_g wavefunction for short chains.

In addition to the purely theoretical interest in understanding the nature of the dark state, there is experimental [16–21] and theoretical [6, 22–27] evidence which suggests that the $2A_g$-family of states might act as intermediates in the formation of uncorrelated triplets during singlet fission in polyenes and carotenoids. In long polyene-type systems there is evidence of triplet formation via singlet fission on single chains [16, 17, 19, 28]. For shorter polyenes, e.g., carotenoids, however, singlet fission appears to occur only in aggregates and dimers [21, 29–33].

View Article Online
DOI: 10.1039/D6CP01090C

There is some controversy as to whether or not singlet fission in carotenoid aggregates proceeds via an intramolecular singlet triplet-pair intermediate. On one hand, some researchers [21, 32] argue that the initially photoexcited singlet state interconverts into a intramolecular singlet triplet-pair. This mechanism proposes that there is a relaxation pathway from the bright state to one of the triplet-pair dark states, which in turn can (in an aggregate) unbind and decohere into two separate triplet excitations. The spectroscopic observation of an intermediate state, often labelled S^*, is evidence in favour of this relaxation pathway. On the other hand, there is some evidence [30, 33, 34] to suggest that singlet fission instead is facilitated by charge-transfer states, with or without an observable (singlet) intermediate state. This implies that the mechanism in carotenoids is similar to the one applicable in polyacenes, which proceeds via coupling of both intermolecular triplet-pairs and initial singlet state to higher energy charge-transfer states [35, 36]. The ambiguity in possible mechanisms is not helped by the practical and theoretical difficulties of studying carotenoid aggregates - for example, heterogeneous aggregates [37] make spectroscopical data difficult to interpret, whilst systems larger than two chains are not easily simulated using current ab initio methods. Furthermore, it is possible that both suggested mechanisms are viable [23], but one is significantly slower than the other depending on the specific system.

To help elucidate the singlet fission mechanism in polyenes and carotenoids, it is necessary to quantify the triplet-pair character of the dark states. In this paper we achieve this goal by solving the Pariser-Parr-Pople (PPP) model of π-electron systems using the density matrix renormalisation group (DMRG) method [38–41]. The triplet-pair population of the 2^1A_g state as a function of the Coulomb interaction is computed by exploiting the MPS structure [42] of the DMRG wavefunction. Our rigorous DMRG solution of the PPP model means that the highly-correlated 2^1A_g state is correctly described. Moreover, our real-space projection technique computes a triplet-pair population that is relevant to the expected triplet yield from singlet fission.

The contents of this paper are as follows. Section II contains the theoretical details. We begin by describing the PPP model (in Section II A), and reprising the DMRG method and MPS formulation (in Section II B). Next, in Section II C we motivate our definition of the triplet-pair population of the 2^1A_g state by describing an exact calculation of the two-particle population of a toy model that describes two-particle interactions. This method is adapted in Section II D to calculate the triplet-pair population of the 2^1A_g state computed

View Article Online
DOI: 10.1039/D6CP01090C

using DMRG from the PPP model. Our results are described in Section III and we conclude in Section IV.

II. THEORY

A. The Pariser-Parr-Pople model

The Pariser-Parr-Pople (or extended Hubbard) Hamiltonian for a linear chain of N C-atoms is defined as

$$\begin{aligned} \hat{H}_{PPP} = \quad & -\sum_{i\sigma}^{N-1} t_i \left(\hat{c}^{\dagger}_{i\sigma} \hat{c}_{i+1\sigma} + \hat{c}^{\dagger}_{i+1\sigma} \hat{c}_{i\sigma} \right) + U \sum_{i} \left(\hat{N}_{i\uparrow} - \frac{1}{2} \right) \left(\hat{N}_{i\downarrow} - \frac{1}{2} \right) \\ & + \sum_{i} \sum_{j \geq i} V_{ij} \left(\hat{N}_i - 1 \right) \left(\hat{N}_j - 1 \right) . \end{aligned} \quad (1)$$

The operator $\hat{c}^{\dagger}_{i\sigma}$ ($\hat{c}_{i\sigma}$) creates (destroys) an electron with spin σ in the p_z orbital on C-atom i. The hopping of the electrons between neighbouring atoms is defined by the transfer integral t_i, where for periodic bond alternation we define $t_d = t_0(1+\delta)$ and $t_s = t_0(1-\delta)$ as the double- and single-bond hopping integrals, respectively. The Coulomb interaction is modelled using the semi-empirical Ohno potential,

$$V_{ij} = \frac{U}{\sqrt{1 + (U \epsilon r_{ij}/14.397)^2}}, \quad (2)$$

where the Coulomb parameter U is in eV, ϵ is the relative permittivity and r_{ij}, the distance between electrons on C-atoms i and j, is in Å. We vary U between 4-14 eV, range which includes the typical values of the Coulomb parameter used for π-conjugated systems [6, 43]. For all calculations that we discuss next, we have taken $\epsilon = 2$, $t_0 = 2.4$ eV and $\delta = 1/12$, so that $t_d = 2.6$ eV and $t_s = 2.2$ eV. Fig. S1 in Supporting Information shows a comparison between our choice of parameters, ab initio DMRG and experimental results.

B. DMRG and the MPS representation

We use the Density Matrix Renormalisation Group (DMRG) method [38–40] to solve the PPP Hamiltonian. The DMRG algorithm accurately and efficiently truncates the Hilbert

View Article Online
DOI: 10.1039/D6CP01090C

space, and is especially well-suited at solving one-dimensional problems [6, 40, 44–47] due to the rapid exponential decay of the eigenspectrum of the density matrix. In our case, we first employ the use of the infinite chain algorithm to grow the chain to the desired length. Afterwards, one iteration of the finite chain algorithm (i.e., a sweep) is enough to assure that the solutions of Eq. 1 converged (Table S1 in Supporting Information shows the results of convergence testing).

The wavefunctions obtained from DMRG [38, 39] are of the form

$$|\Psi_N\rangle = \sum_{\alpha_n \sigma_{n+1} \sigma_{n+2} \beta_{n+2}} \Psi_{\alpha_n \sigma_{n+1} \sigma_{n+2} \beta_{n+2}} |\alpha_n\rangle |\sigma_{n+1}\rangle |\sigma_{n+2}\rangle |\beta_{n+2}\rangle, \tag{3}$$

where the state $|\sigma_m\rangle$ describes the mth C-atom in a chain of N C-atoms, and the block states $|\alpha_n\rangle$ and $|\beta_{n+2}\rangle$ describe the two DMRG blocks, as shown in Fig. 1. We can view DMRG wavefunctions via the Matrix Product State (MPS) formalism [41, 42], which allows us to write the block states as a linear combination of tensor products,

$$|\alpha_n\rangle = \sum_{\alpha_1, \alpha_2, \ldots, \alpha_{n-1}} \sum_{\sigma_1, \sigma_2, \ldots, \sigma_n} A^{\sigma_1}_{\alpha_1} A^{\sigma_2}_{\alpha_1, \alpha_2} \ldots A^{\sigma_n}_{\alpha_{n-1}, \alpha_n} |\sigma_1 \sigma_2 \ldots \sigma_n\rangle, \tag{4}$$

where $A^{\sigma_m}_{\alpha_{m-1}, \alpha_m}$ is the MPS tensor corresponding to the mth C-atom in the left block. Likewise, the states describing the right block are

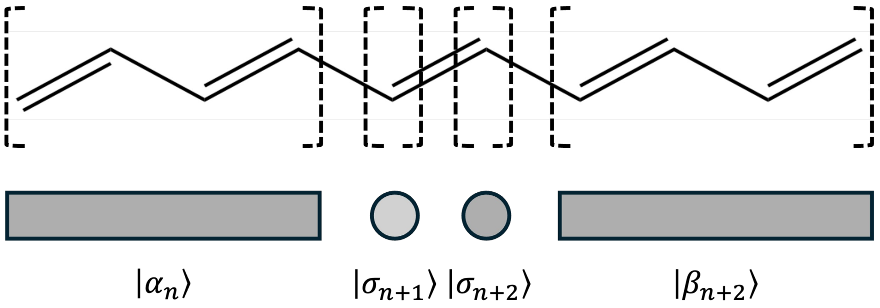

FIG. 1. The structure of the DMRG blocks. The first and last blocks are described by the set of block states $\{|\alpha_n\rangle\}$ and $\{|\beta_{n+2}\rangle\}$ respectively, which correspond to linear combinations of tensor products of site states, $|\sigma_m\rangle$. Above the block diagram is a representation of the respective segments of a real chain that these block states describe. The site states describe the occupation of the carbon p_z orbitals, i.e., $|\sigma\rangle = \{|0\rangle, |\uparrow\rangle, |\downarrow\rangle, |\uparrow\downarrow\rangle\}$.

View Article Online
DOI: 10.1039/D6CP01090C

$$|\beta_{n+2}\rangle = \sum_{\beta_{n+3},\ldots,\beta_{N-2},\beta_{N-1}} \sum_{\sigma_{n+3},\ldots,\sigma_{N-1},\sigma_N} B^{\sigma_{n+3}}_{\beta_{n+2},\beta_{n+3}} \ldots B^{\sigma_{N-1}}_{\beta_{N-2},\beta_{N-1}} B^{\sigma_N}_{\beta_{N-1}} |\sigma_{n+3} \ldots \sigma_{N-1}\sigma_N\rangle, \quad (5)$$

where $B^{\sigma_m}_{\beta_{m-1},\beta_m}$ is the MPS tensor corresponding to the mth C-atom in this block.

This form of the wavefunction is of better use to us, as it allows us to compute wavefunction overlaps straight-forwardly [41]. We can always write all wavefunctions in the same (site) basis, irrespective of the truncation procedure or rotation of the block basis involved in DMRG.

C. Two-particle representation of the triplet-pair state

In this section we motivate our procedure to determine the triplet-pair population of the 2^1A_g state. We do this by the simpler problem of computing the two-particle population of a general many-particle eigenstate of the Hamiltonian $\hat{H} = \hat{H}_1 + \hat{H}_2$, where

$$\hat{H}_1 = -t \sum_{n=1}^{N_d-1} |n\rangle\langle n+1| + |n+1\rangle\langle n|, \quad (6)$$

and

$$\hat{H}_2 = -V \sum_{n=1}^{N_d-1} |n; n+1\rangle\langle n; n+1|. \quad (7)$$

$\hat{H}_1$ describes the hopping of indistinguishable particles between neighbouring sites along a linear chain of N_d sites, while $\hat{H}_2$ describes a nearest-neighbour two-particle interaction. We assume a hard-core repulsion between the particles. (The nearest-neighbour attraction in Eq. (7) is motivated by the derivation in Ref. [5] of a nearest-neighbour triplet-triplet attraction in polyenes mediated by a charge-transfer exciton. However, the method described in this section is general and it equally works for $\hat{H}_2 = \sum_{m \neq n} V_{mn} |m,n\rangle\langle m,n|$ for any interaction V_{mn}.)

We construct a two-particle basis of size $N_d(N_d-1)/2$ for a chain of N_d sites composed of two subchains of length m and $(N_d - m)$ by a tensor product of the one-particle states, as illustrated in Fig. 2. The tensor product is defined as

$$|TT_j(m)\rangle = |T_j(m)\rangle \otimes |T_1(N_d - m)\rangle, \quad (8)$$

View Article Online
DOI: 10.1039/D6CP01090C

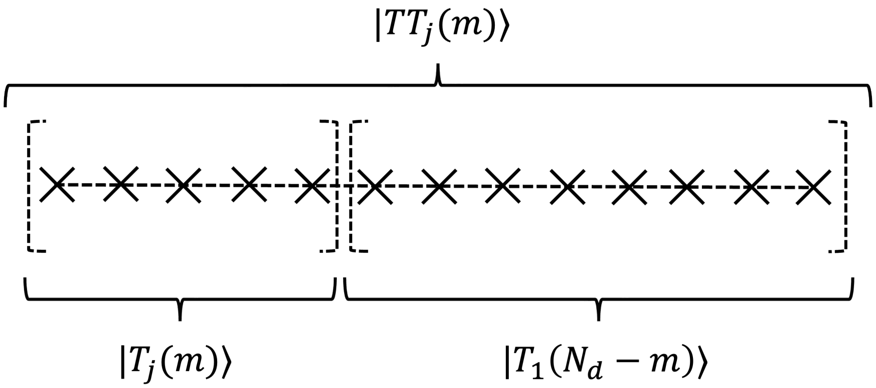

FIG. 2. The definition of our two-particle (or triplet-pair) basis, described in Section II C (and Section II D). × represents a site (or dimer). For a chain of N_d sites (or dimers), we define a two-particle (or triplet-pair) state as the tensor product between a single-particle (or triplet) state $|T_j(m)\rangle$ occupying the left subchain of m sites (or dimers) and a single-particle (or triplet) state $|T_1(N_d - m)\rangle$ occupying the right subchain of $(N_d - m)$ sites (or dimers). $1 \le m \le (N_d - 1)$ and $1 \le j \le m$, such that $\sum_{m=1}^{N_d-1} m = N_d(N_d-1)/2$.

where

$$|T_j(m)\rangle = \left(\frac{2}{m+1}\right)^{1/2} \sum_{n=1}^{m} \sin\left(\frac{\pi j n}{m+1}\right) |n\rangle \tag{9}$$

is a one-particle eigenstate of $\hat{H}_1$ for a subchain of m sites. The length of the left-hand subchain, m, satisfies $1 \le m \le (N_d - 1)$, while the quantum number j satisfies $1 \le j \le m$, such that the basis $\{|TT_j(m)\rangle\}$ spans the complete two-particle Hilbert space, i.e., $\sum_{m=1}^{N_d-1} m = N_d(N_d-1)/2$.

Next, the basis $\{|TT_j(m)\rangle\}$ is orthonomalized via the Löwdin symmetric orthogonalization [48] procedure to yield the basis $\{|\mathcal{TT}_j(m)\rangle\rangle\}$ (denoted by the double-ket).

We explicitly demonstrate numerically that this basis is a complete representation of any two-particle eigenstate, $|\Psi\rangle$, of $\hat{H}$ by computing the population,

$$P = \sum_{m=1}^{N_d-1} \sum_{j=1}^{m} |\langle\langle \mathcal{TT}_j(m)|\Psi\rangle|^2 \,. \tag{10}$$

$P = 1$ for value choice of the interaction, V, or for any state $|\Psi\rangle$.

View Article Online
DOI: 10.1039/D6CP01090C

D. Definition of the triplet-pair population of the 2^1A_g state

The mapping of the two-particle problem described in Section II C onto the calculation of the triplet-pair population of the 2^1A_g state is by the observation that the ket $|n\rangle$ in Eq. (9) represents a triplet localized on the nth ethylene-dimer. In addition, $|T_j(m)\rangle$ represents a triplet eigenstate on a subchain of m dimers with j labelling the state in ascending energy. Finally, the two-particle state $|\Psi\rangle$ represents the 2^1A_g state of the full chain of N_d dimers. Both the triplet and 2^1A_g states are now computed from the PPP model via DMRG. For a subchain of m dimers $|T_j(m)\rangle$ is selected from the m members of the lowest-lying covalent triplet family, i.e., those with the same particle-hole symmetry as the 2^1A_g state.

We then use the MPS representation of the DMRG wavefunction to compute the tensor product

$$|TT_j(m)\rangle = |T_j(m)\rangle \otimes |T_1(N_d - m)\rangle, \tag{11}$$

where $1 \leq m \leq (N_d - 1)$ and $1 \leq j \leq m$, again illustrated in Fig. 2. We next orthonormalize these triplet-pair states via the Löwdin orthogonalization [48] to yield the basis $\{|TT_j(m)\rangle\rangle\}$ and again using the MPS formulation we compute the projection $\langle\langle TT_j(m)|2^1A_g\rangle$.

The triplet-pair population, P_{TT}, of the 2^1A_g state is now defined as

$$P_{TT} = 3\sum_{m=1}^{N_d-1}\sum_{j=1}^{m}\left|\langle\langle TT_j(m)|2^1A_g\rangle\right|^2, \tag{12}$$

where the factor of 3 appears because we only compute triplet-pairs where the triplets in both subchains have a spin-projection, $S_z = 0$, i.e., the triplet-pairs are $T_0 \otimes T_0$, where the subscript refers to the m_S quantum number of that triplet. A triplet-pair in an overall singlet state is

$$|^1TT\rangle = \frac{1}{\sqrt{3}}\left(|T_{+1}T_{-1}\rangle - |T_0T_0\rangle + |T_{-1}T_{+1}\rangle\right). \tag{13}$$

Since the 2^1A_g state is a spin eigenstate with $S = 0$ eigenvalue, it must be the case that any triplet-pair component will be found in an overall spin-symmetrised singlet state. It follows that

$$\left|\langle^1TT|2^1A_g\rangle\right|^2 = \frac{1}{3}\left|\langle T_{+1}T_{-1}|2^1A_g\rangle - \langle T_0T_0|2^1A_g\rangle + \langle T_{-1}T_{+1}|2^1A_g\rangle\right|^2, \tag{14}$$

where the overlap integrals satisfy

$$\langle T_{+1}T_{-1}|2^1A_g\rangle = -\langle T_0T_0|2^1A_g\rangle = \langle T_{-1}T_{+1}|2^1A_g\rangle \tag{15}$$

View Article Online
DOI: 10.1039/D6CP01090C

due to the overall singlet spin multiplicity of the 2^1A_g state, as mentioned above. Therefore, the triplet-pair population can be written as

$$\left|\langle {}^1TT|2^1A_g\rangle\right|^2 = 3\left|\langle T_0T_0|2^1A_g\rangle\right|^2, \tag{16}$$

which is Eq. (12).

In addition to the triplet-pair population, we also calculate the triplet-pair binding energy, ΔE_{TT}, defined as

$$\Delta E_{TT} = E_{1^5A_g} - E_{2^1A_g}. \tag{17}$$

We use the energy of the lowest quintet state 1^5A_g as a proxy for the energy of two electronically uncorrelated triplets. Based on an energetics argument, Valentine et al. [6] suggested that the lowest quintet state in polyenes has predominantly unbound triplet-pair character. We calculate the triplet-pair population of the lowest quintet state for chains of 8, 10, 12 and 14 C-atoms, i.e., $N_d = 4$, 5, 6 and 7 ethylene dimers respectively) for all values of the Coulomb interaction parameter considered. The triplet-pair population of the quintet state is defined analogously to Eq. 12:

$$P_{TT}^{Q} = \frac{3}{2}\sum_{m,j}\left|\langle\langle TT_j(m)|1^5A_g\rangle\right|^2, \tag{18}$$

where the factor of 3/2 arises by the same argument as above, with the quintet state defined as

$$|{}^5TT\rangle = \frac{1}{\sqrt{6}}\left(|T_{+1}T_{-1}\rangle + 2|T_0T_0\rangle + |T_{-1}T_{+1}\rangle\right). \tag{19}$$

Calculations of the triplet-pair population of the quintet state, as well as the next lowest energy dark state, 1^1B_u, are discussed in Appendix A. In all cases, $P_{TT}^{Q} \gtrsim 90\%$, which is further evidence that the quintet state does indeed correspond to a pair of unbound triplets.

Notice that although the two-particle basis defined in Section II C is complete, it does not necessarily follow that our triplet-pair basis constructed from the DMRG calculation of the PPP model is also complete. Therefore, our calculated triplet-pair population is formally a lower bound. This is confirmed by our estimate of the triplet-pair population of the lowest energy quintet state of the PPP model as being only ca. 93%, rather than 100%. However, as noted by previous authors [6, 13, 45], the $|T_1 \otimes T_1\rangle$ triplet-pairs are expected to form the largest contribution to the 2^1A_g state. Our triplet-pair basis accounts for every partition

View Article Online
DOI: 10.1039/D6CP01090C

of a chain into two T_1 triplet states, with smaller contributions from higher energy triplet-pairs. Therefore, the triplet-pair population of the 2^1A_g state as calculated in this paper is expected to account for almost all of the triplet-pair character of the dark state.

III. RESULTS

The calculated values of P_{TT} as a function of the Coulomb parameter, U, are shown in Fig. 3(a). The triplet-pair population increases with increasing Coulomb interaction, reaching the asymptotic limit of $P_{TT} \to 1$ as $U/t_0 \to \infty$ for all chain lengths. That the 2^1A_g state becomes entirely triplet-pair in character in the strong-coupling limit is a known result [3–5]. In this limit, all determinants corresponding to each p_z-orbital that are singly occupied by an electron are degenerate [11], meaning that there are 2^N degenerate eigenstates with the same energy as the 1^1A_g state, including the 2^1A_g state. The 2^1A_g state corresponds to two electron spin flips with respect to 1^1A_g [4, 13]. Since there are no charge-transfer components, this implies that the 2^1A_g state is entirely triplet-pair in character.

On the other hand, we note that the triplet-pair population does not vanish in the opposite, noninteracting limit, as one might expect from the molecular orbital description. As shown in Appendix B and Ref. [3], contributions to the ground state from charge-transfer states between ethylene dimers result a in nonzero triplet-pair character in the 2^1A_g state. This is a consequence of using the real-space valence bond picture to analyse the noninteracting eigenstates. Within the molecular orbital (or band) picture the 2^1A_g state is a single electron-hole (e-h) excitation, i.e., the 2^1A_g state does not have any doubly-excited e-h character in the noninteracting limit. Furthermore, the growth of the triplet-pair character with increasing Coulomb interaction is a consequence of the covalent states (i.e., triplet-pairs) becoming more energetically favourable with respect to the ionic contributions (i.e., charge-transfer excitons) in the 2^1A_g state [3–5].

The dependence of P_{TT} on chain length is shown in Fig. 3(b). We notice an increase in P_{TT} with increasing number of C-atoms, N, but no obvious relationship emerges between the triplet-pair population and the size of the system from our data. We fitted our data to the power function $P_{TT}(N) = aN^{-\alpha} + c$. We see that this predicts a monotonic increase in the triplet-pair population of the 2^1A_g state with increasing number of C-atoms. This behavior correlates with the change in the binding energy, shown in Fig. 4. The triplet-pair binding

View Article Online
DOI: 10.1039/D6CP01090C

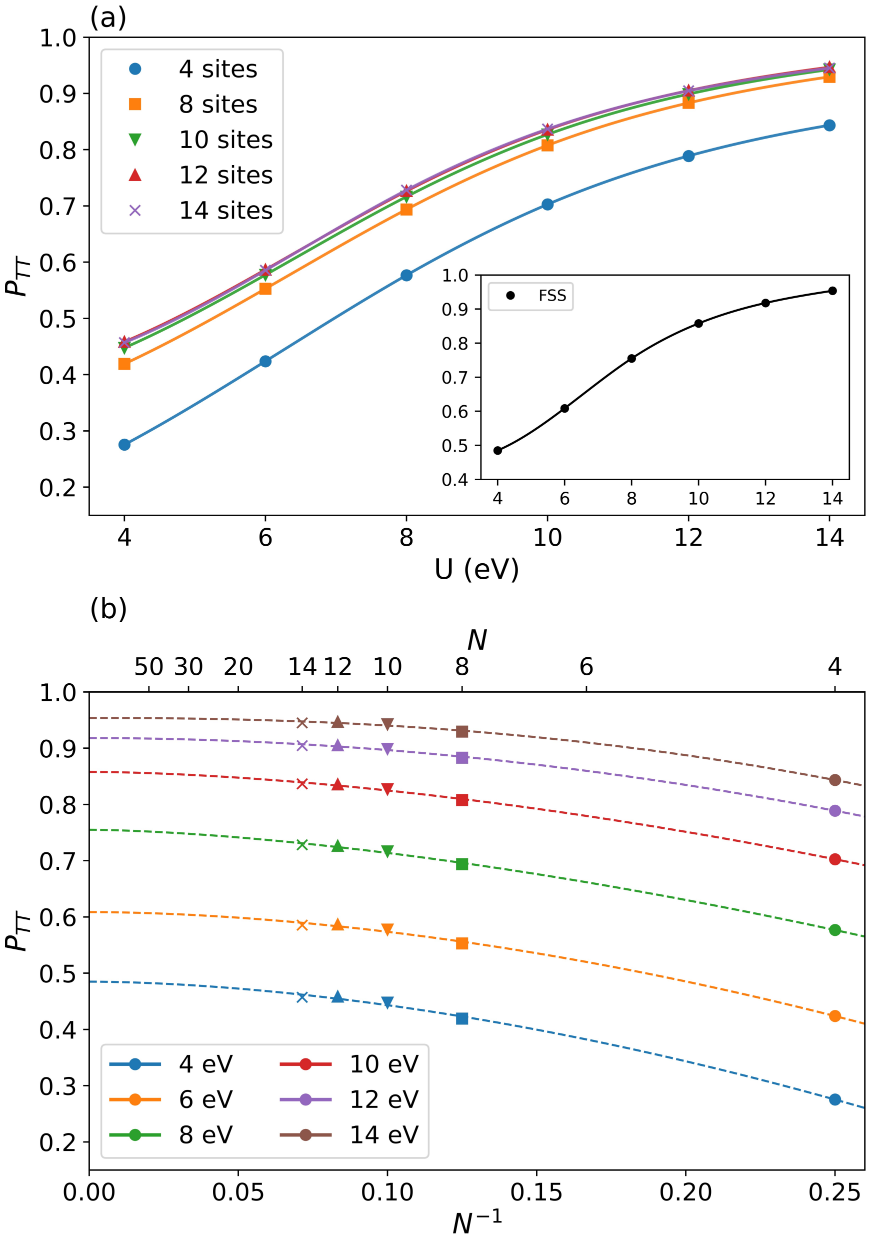

FIG. 3. (a) The triplet-pair population, P_{TT}, of the 2^1A_g state (defined in Eq. (12)) as a function of the Coulomb interaction parameter, U. (b) The extrapolation of the finite-size-scaling (FSS) values of P_{TT} for the six different Coulomb parameters versus N^{-1}, where N is the number of C-atoms. The data was fitted to the function $P_{TT} = aN^{-\alpha} + c$. The inset in (a) shows the FSS values of P_{TT} as a function of U. Also shown are the exact values of P_{TT} for a 4 C-atom chain, as described in Appendix B.

energy and the triplet-pair population are related quantities: P_{TT} increases with decreasing ΔE_{TT} [5]. The finite-size-scaling (FSS) result for the triplet-pair population as a function

View Article Online
DOI: 10.1039/D6CP01090C

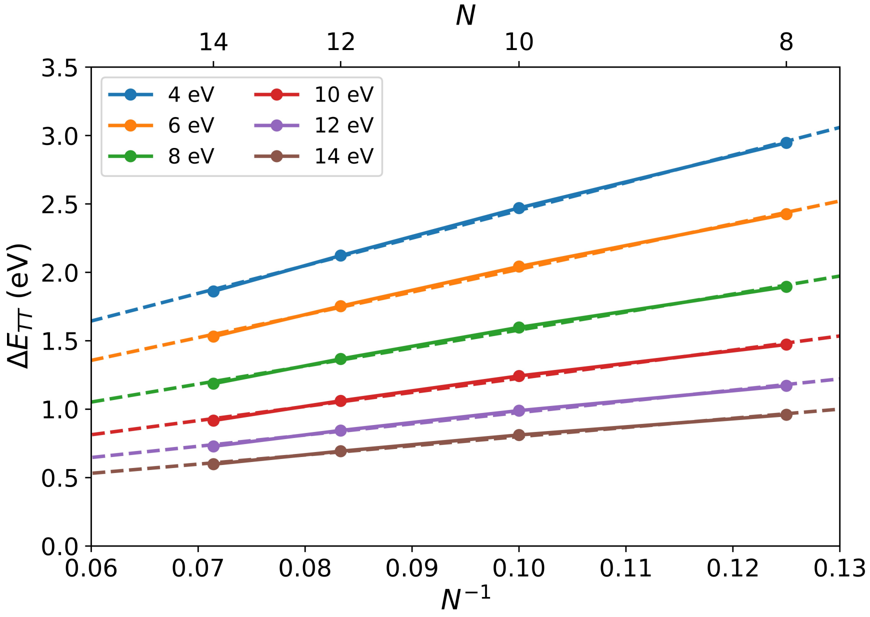

FIG. 4. The triplet-pair binding energy, ΔE_{TT}, (defined in Eq. (17)) as a function of N^{-1}, where N is the number of C-atoms, for different values of the Coulomb parameter, U.

of Coulomb interaction is shown in the inset of Fig. 3(a). As shown in the SI, the realistic value of U for π-conjugated systems [43] is ca. 8 eV, and thus we deduce that the triplet-pair population, P_{TT}, in polyenes is ca. 75%. Note that this value, although remarkably close to the calculated values of the doubly-excited character of the 2^1A_g state [9, 10], does not necessarily imply that the 2^1A_g state has 75% doubly-excited character, as shown in Appendix B for the noninteracting limit. The triplet-pair population is a quantity closely related to the doubly-excited character (i.e., the weight of the doubly-excited determinants) of a wavefunction but not equivalent to it, as one is defined within real space and the other within the molecular orbital theory. However, both are seen to follow similar trends [7–10].

View Article Online
DOI: 10.1039/D6CP01090C

IV. DISCUSSION AND CONCLUSIONS

In conclusion, we have presented the results of numerical calculations of the real-space triplet-pair population of polyenes of 8, 10, 12, and 14 C-atoms for different values of the Coulomb interaction. Using these results and the correlation between the triplet-pair binding energy and triplet-pair character of the 2^1A_g state, we extrapolated the value of the triplet-pair population to infinitely long chains. Our calculations agree with other measures of double-excitation character derived from ab initio calculations [7–10], where an increase in the triplet-pair character with increasing chain size is observed. Furthermore, we notice that the triplet-pair population also agrees with calculations of Chandross et al. [3] in the limit of noninteracting electrons where P_{TT} is small but nonzero, as well as in the strongly-interacting limit where the 2^1A_g state $P_{TT} \to 1$.

Our results have implications for possible singlet-fission mechanisms in carotenoids that postulate that one of the 2^1A_g-family [6] is the intermediary between the bright-excited state and spatially uncorrelated, decohered triplet-pairs. However, since the lowest-energy member of this family (i.e., the 2^1A_g state) is composed of a strongly bound triplet-pair [5, 6], potential singlet fission from this state would be endothermic, whereas potential singlet fission from higher-energy members would be exothermic [6, 25]. The triplet-pair population of these higher-energy members of the 2^1A_g-family are therefore discussed in Appendix A.

ACKNOWLEDGMENTS

A.G.I. thanks Linacre College for the Carolyn and Franco Gianturco Scholarship.

CONFLICTS OF INTEREST

The authors do not have any conflicts of interest to disclose.

SUPPORTING INFORMATION

1. PPP Model Parametrisation, 2. DMRG Convergence Tests

View Article Online
DOI: 10.1039/D6CP01090C

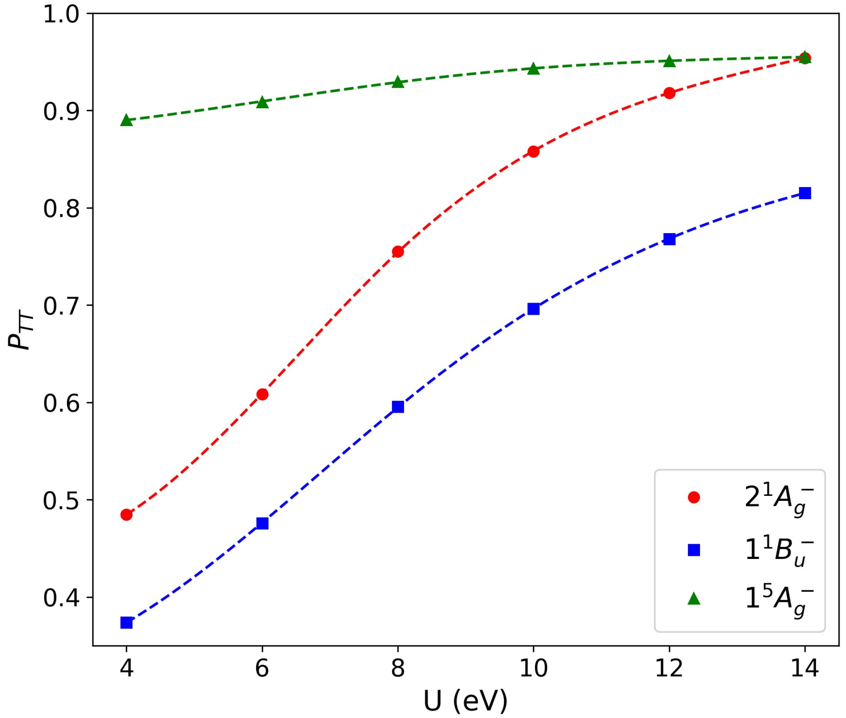

FIG. 5. The triplet-pair population of the first and second lowest energy dark states, $2^1A_g^-$ and $1^1B_u^-$, in the limit of infinite chains. Also shown is the triplet-pair population calculated for the lowest energy quintet state, $1^5A_g^-$.

Appendix A: Triplet-pair population of the $2A_g$-family of states

The $2^1A_g^-$ state is the lowest energy member (with the lowest pseudomomentum) of a band of states that corresponds to the triplet-pair quasiparticle [6]. The higher-energy (higher pseudomomentum) states are $1^1B_u^-, 3^1A_g^-, \cdots$. Here, we explicitly label the states using the particle-hole notation for covalent ("-") and ionic ("+") states so as to distinguish the $1^1B_u^-$ state from the optically bright $1^1B_u^+$ state.

As discussed in Section IV, although the $2^1A_g^-$ state has a large triplet-pair population, singlet-fission from this state would be endothermic, owing to the strong triplet-pair attraction [5, 6]. In contrast, triplets in the higher-energy members of the 2^1A_g-family are weakly bound and intermolecular singlet-fission from these states would be exothermic [6, 25]. Thus, the triplet-pair population of these states is relevant for potential singlet-fission mechanisms in polyenes.

Fig. 5 shows the triplet-pair population of the $2^1A_g^-$ and $1^1B_u^-$ states, in the limit of

View Article Online
DOI: 10.1039/D6CP01090C

infinite chains (as predicted in the same way as described in the main text). The triplet-pair population is observed to decrease as the pseudomomentum increases, i.e., higher energy dark states have a smaller P_{TT}. This can be rationalized by the coupling between the singlet triplet-pair subspace and the higher energy singlet charge-transfer exciton subspace, as described in Ref. [5]. This coupling results in a series of eigenstates, where the lowest energy eigenstate has the highest triplet-pair weight. Furthermore, our result agrees with the ab initio prediction in Ref. [9] that the doubly-excited character of the $1^1B_u^-$ state is smaller than that of $2^1A_g^-$ state. (The spin correlations and charge-transfer exciton wavefunctions of the $2^1A_g^-$, $1^1B_u^-$ and $3^1A_g^-$ members of the 2^1A_g-family are illustrated in Fig. 7 and Fig. 8 of Ref. [6], respectively.)

The extrapolated triplet-pair population of the lowest quintet state, $1^5A_g^-$, is also shown in Fig. 5. For a chain of 4 C-atoms, a quintet state can only be formed by the coupling of two triplet states in an overall $S = 2$ state. Therefore, for butadiene, this quintet state has $P_{TT}^Q = 1$. Applying our definition of P_{TT}^Q for chains of 8 to 14 C-atoms we find $0.90 \leq P_{TT}^Q \leq 0.96$, where the triplet-pair population increases with increasing Coulomb parameter and decreases with increasing chain length.

Appendix B: Triplet-pair population in the noninteracting limit

In this appendix we demonstrate that in the noninteracting limit in a chain of four C-atoms (i.e., sites) the 2^1A_g state has a nonzero triplet-pair population.

The noninteracting π-electron Hamiltonian is

$$\hat{H} = -\sum_{i,\sigma} t_i(\hat{c}_{i\sigma}^\dagger \hat{c}_{i+1\sigma} + \hat{c}_{i+1\sigma}^\dagger \hat{c}_{i\sigma}), \tag{B1}$$

where $t_i = t_0(1 + (-1)^{(i+1)}\delta)$ and we take $\delta = 1/12$.

On a chain of four-sites the 2^1A_g state written in the site basis is

$$|2^1A_g\rangle = 0.1794\,(|\uparrow\downarrow\uparrow\downarrow\rangle + |\downarrow\uparrow\downarrow\uparrow\rangle - |\downarrow\downarrow\uparrow\uparrow\rangle - |\uparrow\uparrow\downarrow\downarrow\rangle) + \ldots, \tag{B2}$$

where we only show the covalent (i.e., singly occupied site) contributions to the state.

Partitioning the four-site chain into two subchains of two sites each, we can write the triplet states of each subchain (or dimer) as

$$|T_{+1}\rangle = |\uparrow\uparrow\rangle, \tag{B3}$$

View Article Online
DOI: 10.1039/D6CP01090C

$$|T_0\rangle = \frac{1}{\sqrt{2}} \left(| \uparrow\downarrow \rangle + | \downarrow\uparrow\rangle \right) \tag{B4}$$

and

$$|T_{-1}\rangle = | \downarrow\downarrow\rangle, \tag{B5}$$

for the $M_s = +1, 0$ and -1 spin-projections, respectively.

The triplet-pair basis for the four-site (two-dimer) chain that spans the $S_z = 0$ subspace is

$$|T_{+1}T_{-1}\rangle = | \uparrow\uparrow\downarrow\downarrow\rangle, \tag{B6}$$

$$|T_0T_0\rangle = \frac{1}{2} \left(| \uparrow\downarrow\uparrow\downarrow \rangle + | \uparrow\downarrow\downarrow\uparrow\rangle + | \downarrow\uparrow\uparrow\downarrow\rangle + | \downarrow\uparrow\downarrow\uparrow\rangle \right) \tag{B7}$$

and

$$|T_{-1}T_{+1}\rangle = | \downarrow\downarrow\uparrow\uparrow\rangle. \tag{B8}$$

The projection of each of these triplet-pair basis states onto the 2^1A_g state (given in Eq. (B2)) is 0.1794 and thus the total triplet-pair population of this state is 9.66%.

Alternatively, using Eq. (B6), Eq. (B7) and Eq. (B8), we can construct the singlet triplet-pair state for the four-site chain as

$$|^1TT\rangle = \frac{1}{\sqrt{3}} \left(|T_{+1}T_{-1}\rangle - |T_0T_0\rangle + |T_{-1}T_{+1}\rangle \right). \tag{B9}$$

Projecting this state onto the 2^1A_g state, the triplet-pair population is $|\langle ^1TT|2^1A_g\rangle|^2 =$ 9.66%, as before. This value is the exact triplet-pair population because, for a chain of four C-atoms, $|^1TT\rangle$ spans the whole $S = 0$ space of electron configurations that can be written as a product of two triplet states.

The results of the same analysis for the values of the Coulomb parameter considered in the main text are shown in Fig. 3, which shows that the triplet-pair population increases as the Coulomb interaction increases.

---

[1] K. Schulten and M. Karplus, On the origin of a low-lying forbidden transition in polyenes and related molecules, Chemical Physics Letters **14**, 305 (1972).

[2] B. Hudson and B. Kohler, A low-lying weak transition in the polyene α,ω-diphenyloctatetraene, Chemical Physics Letters **14**, 299 (1972).

View Article Online
DOI: 10.1039/D6CP01090C

[3] M. Chandross, Y. Shimoi, and S. Mazumdar, Diagrammatic exciton-basis valence-bond theory of linear polyenes, Phys. Rev. B **59**, 4822 (1999).

[4] W. Barford, *Electronic and Optical Properties of Conjugated Polymers*, 2nd ed. (Oxford University Press, 2013).

[5] W. Barford, Theory of the dark state of polyenes and carotenoids, Phys. Rev. B **106**, 035201 (2022).

[6] D. J. Valentine, D. Manawadu, and W. Barford, Higher-energy triplet-pair states in polyenes and their role in intramolecular singlet fission, Phys. Rev. B **102**, 125107 (2020).

[7] M. T. do Casal, J. M. Toldo, M. Barbatti, and F. Plasser, Classification of doubly excited molecular electronic states, Chem. Sci. **14**, 4012 (2023).

[8] J. C. V. Chagas, L. G. F. dos Santos, R. Nieman, A. J. A. Aquino, S. A. do Monte, F. Plasser, P. G. Szalay, H. Lischka, and F. B. C. Machado, Low-lying excited states of linear all-trans polyenes: the σ–π electron correlation and the description of ionic states, Phys. Chem. Chem. Phys. **27**, 7916 (2025).

[9] J. H. Starcke, M. Wormit, J. Schirmer, and A. Dreuw, How much double excitation character do the lowest excited states of linear polyenes have?, Chemical Physics **329**, 39 (2006).

[10] K. Boguslawski, Targeting doubly excited states with equation of motion coupled cluster theory restricted to double excitations, Journal of Chemical Theory and Computation **15**, 18 (2019).

[11] K. Schulten, I. Ohmine, and M. Karplus, Correlation effects in the spectra of polyenes, Journal of Chemical Physics **64**, 4422 (1976).

[12] G. W. Hayden and E. J. Mele, Correlation effects and excited states in conjugated polymers, Phys. Rev. B **34**, 5484 (1986).

[13] P. Tavan and K. Schulten, Electronic excitations in finite and infinite polyenes, Phys. Rev. B **36**, 4337 (1987).

[14] R. J. Bursill and W. Barford, Electron-lattice relaxation, and soliton structures and their interactions in polyenes, Phys. Rev. Lett. **82**, 1514 (1999).

[15] W. Barford, R. J. Bursill, and M. Y. Lavrentiev, Density-matrix renormalization-group calculations of excited states of linear polyenes, Phys. Rev. B **63**, 195108 (2001).

[16] B. Kraabel, D. Hulin, C. Aslangul, C. Lapersonne-Meyer, and M. Schott, Triplet exciton generation, transport and relaxation in isolated polydiacetylene chains: subpicosecond pump-

View Article Online
DOI: 10.1039/D6CP01090C

probe experiments, Chemical Physics **227**, 83 (1998).

[17] G. Lanzani, S. Stagira, G. Cerullo, S. De Silvestri, D. Comoretto, I. Moggio, C. Cuniberti, G. F. Musso, and G. Dellepiane, Triplet exciton generation and decay in a red polydiacetylene studied by femtosecond spectroscopy, Chemical Physics Letters **313**, 525 (1999).

[18] C. Wang and M. J. Tauber, High-yield singlet fission in a zeaxanthin aggregate observed by picosecond resonance raman spectroscopy, Journal of the American Chemical Society **132**, 13988 (2010).

[19] A. J. Musser, M. Al-Hashimi, M. Maiuri, D. Brida, M. Heeney, G. Cerullo, R. H. Friend, and J. Clark, Activated singlet exciton fission in a semiconducting polymer, Journal of the American Chemical Society **135**, 12747 (2013).

[20] A. J. Musser and J. Clark, Triplet-pair states in organic semiconductors, Annual Review of Physical Chemistry **70**, 323 (2019).

[21] A. Kundu and J. Dasgupta, Photogeneration of long-lived triplet states through singlet fission in lycopene h-aggregates, Journal of Physical Chemistry Letters **12**, 1468 (2021).

[22] H. Kim and P. M. Zimmerman, Coupled double triplet state in singlet fission, Physical Chemistry Chemical Physics **20**, 30083 (2018).

[23] S. Santra, J. Ray, and D. Ghosh, Mechanism of singlet fission in carotenoids from a polyene model system, Journal of Physical Chemistry Letters **13**, 6800 (2022).

[24] W. Barford and C. A. Chambers, Theory of singlet fission in carotenoid dimers, Journal of Chemical Physics **159**, 084116 (2023).

[25] W. Barford, Singlet fission in lycopene h-aggregates, Journal of Physical Chemistry Letters **14**, 9842 (2023).

[26] A. G. Ichert and W. Barford, Singlet fission in carotenoid dimers – the role of the exchange and dipolar interactions, Phys. Chem. Chem. Phys. **27**, 2371 (2025).

[27] S. Santra and D. Ghosh, Unraveling the geometrical effects on singlet fission of carotenoids: A model perspective, Journal of Physical Chemistry A **129**, 2738 (2025).

[28] D. W. Polak, I. Andrews, E. Salvadori, A. J. Musser, A. Auty, D. Chekulaev, J. A. Weinstein, M. Heeney, and J. Clark, Conjugation length dependence of intramolecular singlet fission in a series of regioregular oligo 3-alkyl(thienylene-vinylene)s, Journal of the American Chemical Society **147**, 662 (2025).

[29] M. T. Trinh, Y. Zhong, Q. S. Chen, T. Schiros, S. Jockusch, M. Y. Sfeir, M. Steigerwald,

View Article Online
DOI: 10.1039/D6CP01090C

C. Nuckolls, and X. Y. Zhu, Intra- to intermolecular singlet fission, Journal of Physical Chemistry C **119**, 1312 (2015).

[30] A. J. Musser, M. Maiuri, D. Brida, G. Cerullo, R. H. Friend, and J. Clark, The nature of singlet exciton fission in carotenoid aggregates, Journal of the American Chemical Society **137**, 5130 (2015).

[31] M. J. Llansola-Portoles, K. Redeckas, S. Streckaite, C. Ilioaia, A. A. Pascal, A. Telfer, M. Vengris, L. Valkunas, and B. Robert, Lycopene crystalloids exhibit singlet exciton fission in tomatoes, Physical Chemistry Chemical Physics **20**, 8640 (2018).

[32] A. Quaranta, A. Krieger-Liszkay, A. A. Pascal, F. Perreau, B. Robert, M. Vengris, and M. J. Llansola-Portoles, Singlet fission in naturally-organized carotenoid molecules, Physical Chemistry Chemical Physics **23**, 4768 (2021).

[33] B. Peng, Z. Wang, J. Jiang, Y. Huang, and W. Liu, Investigation of ultrafast intermediate states during singlet fission in lycopene h-aggregate using femtosecond stimulated raman spectroscopy, Journal of Chemical Physics **160**, 194304 (2024).

[34] K. Aryanpour, A. Shukla, and S. Mazumdar, Theory of singlet fission in polyenes, acene crystals, and covalently linked acene dimers, Journal of Physical Chemistry C **119**, 6966 (2015).

[35] T. C. Berkelbach, M. S. Hybertsen, and D. R. Reichman, Microscopic theory of singlet exciton fission. II. application to pentacene dimers and the role of superexchange, The Journal of Chemical Physics **138**, 114103 (2013).

[36] T. Zeng, R. Hoffmann, and N. Ananth, The low-lying electronic states of pentacene and their roles in singlet fission, Journal of the American Chemical Society **136**, 5755 (2014).

[37] C. Magne, V. Veremeienko, R. Bercy, M.-H. Ha-Thi, A. A. Arteni, A. A. Pascal, M. Vengris, T. Pino, B. Robert, and M. J. Llansola-Portoles, Singlet fission in heterogeneous lycopene aggregates, Scientific Reports **15**, 5593 (2025).

[38] S. R. White, Density matrix formulation for quantum renormalization groups, Phys. Rev. Lett. **69**, 2863 (1992).

[39] S. R. White, Density-matrix algorithms for quantum renormalization groups, Phys. Rev. B **48**, 10345 (1993).

[40] U. Schollwöck, The density-matrix renormalization group, Rev. Mod. Phys. **77**, 259 (2005).

[41] U. Schollwöck, The density-matrix renormalization group in the age of matrix product states,

View Article Online
DOI: 10.1039/D6CP01090C

Annals of Physics **326**, 96 (2011).

[42] S. Östlund and S. Rommer, Thermodynamic limit of density matrix renormalization, Phys. Rev. Lett. **75**, 3537 (1995).

[43] M. Chandross and S. Mazumdar, Coulomb interactions and linear, nonlinear, and triplet absorption in poly(para-phenylenevinylene), Phys. Rev. B **55**, 1497 (1997).

[44] D. Ghosh, J. Hachmann, T. Yanai, and G. K.-L. Chan, Orbital optimization in the density matrix renormalization group, with applications to polyenes and β-carotene, Journal of Chemical Physics **128**, 144117 (2008).

[45] E. J. Taffet, B. G. Lee, Z. S. D. Toa, N. Pace, G. Rumbles, J. Southall, R. J. Cogdell, and G. D. Scholes, Carotenoid nuclear reorganization and interplay of bright and dark excited states, Journal of Physical Chemistry B **123**, 8628 (2019).

[46] D. Khokhlov and A. Belov, Ab initio study of low-lying excited states of carotenoid-derived polyenes, Journal of Physical Chemistry A **124**, 5790 (2020).

[47] D. Khokhlov and A. Belov, Toward an accurate ab initio description of low-lying singlet excited states of polyenes, Journal of Chemical Theory and Computation **17**, 4301 (2021).

[48] P. Löwdin, On the non-orthogonality problem connected with the use of atomic wave functions in the theory of molecules and crystals, Journal of Chemical Physics **18**, 365 (1950).

The data that supports the findings of this paper are available upon request from the authors.

View Article Online
DOI: 10.1039/D6CP01090C